Nonanalytic crossover behavior of SU($\mathcal{N}_c$) Fermi liquid

Pye Ton How*
Institute of Physics, Academia Sinica, Taipei 115, Taiwan

Sung-Kit Yip†
Institute of Physics, Academia Sinica, Taipei 115, Taiwan
and Institute of Atomic and Molecular Sciences, Academia Sinica, Taipei 106, Taiwan

(Received 18 April 2018; published 26 June 2018)

We consider the thermodynamic potential of a dilute Fermi gas with a contact interaction, at both finite temperature T and nonzero effective magnetic fields $\mathbf{H}$, and derive the equation of state analytically using second-order perturbation theory. Special attention is paid to the nonanalytic dependence of Ω on temperature T and (effective) magnetic field $\mathbf{H}$, which exhibits a crossover behavior as the ratio of the two is continuously varied. This nonanalyticity is due to the particle-hole pair excitation being always gapless and long ranged. The nonanalytic crossover found in this paper can therefore be understood as an analog of the Ginzburg-Landau critical scaling, albeit only at the subleading order. We extend our results to an $\mathcal{N}_c$-component Fermi gas with an SU($\mathcal{N}_c$)-symmetric interaction and point out possible enhancement of the crossover behavior by a large $\mathcal{N}_c$.

DOI: 10.1103/PhysRevA.97.063623

I. INTRODUCTION

The Fermi liquid (FL) paradigm is an important cornerstone of our understanding of nature. It was originally conceived as a phenomenological theory for liquid ^{3}He, but turned out to be generally a good description for most physical systems with fermionic degrees of freedom at low enough temperature. There has long been a consensus [1–14] that the thermodynamic behavior of an FL must be nonanalytic, in contrast to the Ginzburg-Landau (GL) theory, which assumes that the free energy takes an analytic form away from a phase transition. Historically, the specific heat of normal ^{3}He was the earliest experimentally studied example [15,16], where the observed trend cannot be fitted to an analytic function. Theoretical efforts [1,2,4,5,10,13] indicate, to leading order, a $T^3 \ln T$ correction on top of the linear T dependence from the leading-order FL behavior. This nonanalytic correction is a generic feature of any FL, in the sense that it is entirely captured by considering the interaction and scattering between Landau quasiparticles on the Fermi surface. This term has also been studied in the context of heavy fermion metals [17,18]. In ordinary metal, however, it was concluded [19] that the effect will be too small to be observed experimentally.

In the context of an electron liquid, a magnetic field causes a Zeeman split between the two spin components. It was later realized that the magnetic response of an electron liquid is also nonanalytic beyond the leading order [7,10,11,14], with the underlying physics closely related to the temperature case. Theories indicate an $H^2 \ln H$ correction to the constant Pauli susceptibility. In two space dimensions, similar considerations lead to the prediction of a T^2 correction to specific heat and an $|H|$ correction to spin susceptibility [7,8,10,11,14]. This nonanalytic magnetic response has a much more dramatic consequence: It can change the order of the itinerant Ferromagnetic quantum critical point [14,20,21] from second order, as dictated by the GL paradigm, to weakly first order [22].

The particle-hole pair excitation around the Fermi surface has been identified as the cause of this nonanalytic behavior [1,4,13,23]. Such a pair is always gapless in the normal phase. The infrared singularity of the pair's Green's function, while not strong enough to cause a full-fledged divergence, results in the nonanalyticity.

Yet it remains difficult to draw a more precise conclusion beyond the statement that theories and experiments agree qualitatively. Theoretically, even within the Fermi liquid picture, the calculations were usually performed by considering only a subset of all possible interaction processes [1,4,10,23], where the omitted processes solely give rise to analytic terms. One then obtains the nonanalytic term, but on top of an unknown background of analytic contributions. Experimentally, even for the well-studied case of ^{3}He specific heat, the uncertainty in interacting parameters is large enough [24,25] to prevent a more meaningful comparison (see, for example, the discussion of [4,13]). The $H^2 \ln H$ behavior of spin susceptibility has not been observed; however there is experimental evidence of its two-dimensional counterpart: Reference [26] pointed out that the normal state of iron pnictide exhibits a spin susceptibility that increases linearly with temperature [27,28]. This is consistent with the linear nonanalyticity in two dimensions when temperature is dominant, as discussed in [29].

In this paper we theoretically study the nonanalytic effects in the context of a dilute Fermi gas in three space dimensions, in second-order perturbation theory. This choice of theoretical model is made with possible cold-atom experiments in mind.

Experimentally, cold quantum gas has several advantages over other realizations of FL. First of all, the interaction between particles is well approximated by contact

*pthow@gate.sinica.edu.tw
†yip@phys.sinica.edu.tw

interaction and is highly tunable through the Feshbach resonance technique [30] (see [31] for a review). One may realize the weakly interacting dilute limit, amenable to a perturbative treatment. Second, through the use of a nonhomogeneous trap and the local-density approximation, one has direct access to the equation of state of the gas [32–36]. Finally, one is not confined to two-component spin-$\frac{1}{2}$ fermions: Isotopes such as ^{173}Yb and ^{87}Sr have large pseudospins [37–40], which enhance the effects of interaction and potentially make the nonanalytic part more visible experimentally.

At the center of our attention is the thermodynamic potential Ω of the gas. Extending from our previous paper [41], we will study the behavior of Ω using perturbation theory to second order, focusing on the interplay of temperature and magnetic field. In particular, we investigated the crossover between the zero-magnetic-field limit and the zero-temperature limit. We obtain an equation of state for the gas, quantifying both the analytic and the nonanalytic contributions to Ω, thereby facilitating a direct comparison with future experiments.

Since the particle-hole pair excitation is always gapless, it is legitimate to ask if the resultant physics shares any similarities with the usual GL critical phenomenology. We will see that the crossover behavior is strongly reminiscent of a quantum critical point, albeit only at the subleading order. One may claim that a nonmagnetic Fermi liquid is, in a sense, always "critical," regardless of the interaction strength. A similar idea was explored by Belitz *et al.* [42].

II. THERMODYNAMIC POTENTIAL

A. Model Hamiltonian

The $\mathcal{N}_c$-component fermion gas is modeled with anticommuting quantum fields ψ_a, where the index a runs from 1 to $\mathcal{N}_c$. The generalized Zeeman shift in an SU($\mathcal{N}_c$)-invariant theory is given by a traceless Hermitian matrix $\mathbf{H}$, but without loss of generality it may be put into a diagonal form with an appropriate SU($\mathcal{N}_c$) transformation. We therefore write the free Hamiltonian as

$$H_0 = \sum_{a=1}^{\mathcal{N}_c} \int d^3x\, \psi_a^\dagger \left(-\frac{\nabla^2}{2m} - \mu_0 - H_a \right) \psi_a. \tag{1}$$

Here H_a is an eigenvalue of $\mathbf{H}$. The traceless condition of $\mathbf{H}$ translates to $\sum_a H_a = 0$. It is sometimes also convenient to consider the species-dependent effective chemical potential

$$\mu_a \equiv \mu_0 + H_a. \tag{2}$$

We also define the associated momentum scale $k_\mu = \sqrt{2m\mu_0}$ and the analogy of Fermi velocity $v_\mu = k_\mu/m$. To the order of approximation adopted in this paper, these are interchangeable with the actual Fermi momentum and velocity k_F and v_F.

In this paper we will treat μ_0 and $\mathbf{H}$, rather than the fermion number density, as the "tuning knobs" of the system. Experimentally, the (position-dependent) chemical potential of a trapped quantum gas within the local-density approximation is readily available. So we do not see this as a difficulty.

We employ a zero-range interaction

$$H_I = \frac{4\pi a}{m} \sum_{a,b=1}^{\mathcal{N}_c} \int d^3x\, \psi_a^\dagger(x) \psi_b^\dagger(x) \psi_b(x) \psi_a(x). \tag{3}$$

The quantity a is the scattering length of the zero-range two-body potential. We will perform our calculation in the dilute limit, where ak_F is a small expansion parameter. We work in the units $\hbar = k_B = 1$.

Two-particle scattering amplitudes of this model diverge in the Cooper channel. This is the usual pathology of a δ-function potential and can be absorbed by renormalization. In the following we will implicitly assume that all such divergences are removed. Related to this diverging behavior is a pairing instability in the Cooper channel at an exponentially small transition temperature. This instability will be ignored in all subsequent discussion.

Staring from this point, we will consider the case $\mathcal{N}_c = 2$, as the crossover advertised in the beginning is essentially an effect between two spin components. The generalization to a generic $\mathcal{N}_c > 2$ will be discussed later in the paper. For the $\mathcal{N}_c = 2$ case, we denote the two spins $\uparrow$ and $\downarrow$, with the convention $H_\uparrow = H/2$ and $H_\downarrow = -H/2$. Without loss of generality, one can always assume $H \geqslant 0$.

B. Origin of nonanalyticity

For an in-depth discussion of the result quoted in this section, we refer our readers to the work of Chubukov *et al.* [13] and the references therein.

For the $\mathcal{N}_c = 2$ case, the specific heat and spin susceptibility have been shown to receive logarithmic corrections, and the particle-hole pair excitation is solely responsible for the nonanalytic behavior of Ω. As shown in Fig. 1(a), we denote

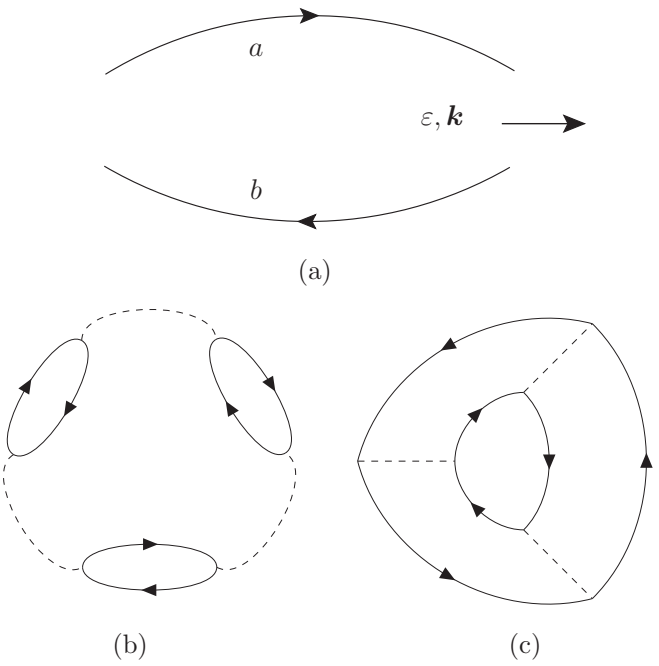

FIG. 1. Feynman diagrams representing (a) the particle-hole bubble $\Pi_{ab}(\varepsilon, \boldsymbol{k})$, (b) an example of a ring diagram with three particle-hole pairs joined together, and (c) an example of a ladder diagram, also with three particle-hole pairs. Note that the spins a and b in Π_{ab} can be different. The low-momentum limit of the ring and ladder diagrams is the origin of the nonanalytic thermodynamic behaviors of a normal Fermi liquid.

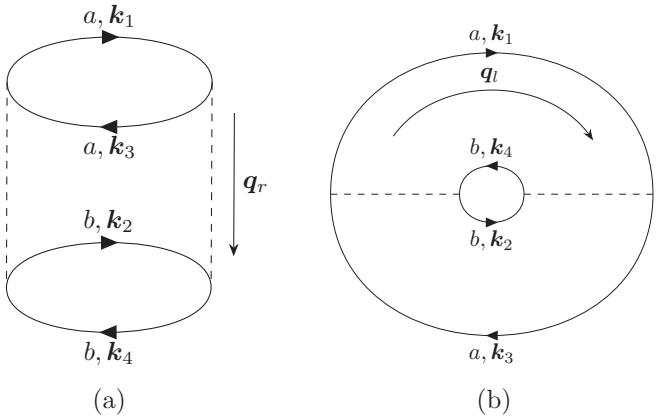

FIG. 2. The same second-order vacuum Feynman diagram can be drawn as either (a) a ring diagram or (b) a ladder diagram. The low-momentum limits of either form correspond to the limit where $\boldsymbol{q}_r = \boldsymbol{k}_1 - \boldsymbol{k}_3$ or $\boldsymbol{q}_l = \boldsymbol{k}_1 - \boldsymbol{k}_4$ vanishes, respectively. This term is labeled Ω_{2a}.

the spins of the particle and hole in such a pair as a and b, respectively, which may or may not be the same. We denote the Green's function for such pair excitation by Π_{ab}.

The thermodynamic potential Ω can be computed by summing over vacuum Feynman diagrams. The pair excitation modes contribute to Ω via two classes of diagrams: the ring diagrams where each bubble consists of the same spin and the ladder diagrams where the particle and hole legs have different spins. Figures 1(b) and 1(c) are examples with three particle-hole pairs.

These pair fluctuation are bosonic and remain soft down to zero momentum. The long-range correlation of these bosonic modes is not strong enough to cause full-fledged infrared divergence in the present case, but results in weaker logarithmic corrections only at higher orders. This is the origin of the nonanalyticity. For a review of this soft-mode paradigm, and in particular how it affects the critical behavior, see [42] and the references therein.

These soft modes must be cut off by some relevant infrared scale. Temperature is an obvious candidate. In the presence of $H_a - H_b \neq 0$, it can be seen that the energy of pair excitation Π_{ab} is shifted by $H_a - H_b$; therefore, the magnetic field can also serve as the cutoff. One expects the larger of the two scales to dominate, and this hints at possible crossover behavior when the ratio T/H is varied continuously between the two extremes [11]. However, each particle-hole pair in the ring diagram is of the same spin and is insensitive to the magnetic field. The crossover behavior is thus exhibited only in the ladder-type nonanalyticity.

In this paper we work to second order in perturbation theory. The ring and ladder diagram at second order is actually one and the same, as shown in Fig. 2. However, the two small-momentum limits refer to distinct regions of the momentum integral.

At second order, the ring diagram is known to yield further nonanalytic terms in the region $q_r \approx 2k_F$ [13]. Historically this has been linked to the dynamic Kohn anomaly [2,4,13]. However, this nonanalytic contribution only comes from the limit where $\boldsymbol{q}_1$ and $\boldsymbol{q}_2$ are antiparallel [2] and can be identified with the small-q_l limit of the ladder diagram [13,14]. Conversely, the ladder diagram also contributes to the nonanalyticity around $q_l \approx 2k_F$ and this translates to the small-q_r limit of the ring diagram. We argue that, rather than the traditional zero-and-$2k_F$ picture, it is more natural to look at the nonanalyticity as coming solely from the zero-momentum limit of particle-hole pairs, but then consider all possible spin combinations.

C. Possible form of Ω

The thermodynamic potential is $\Omega = -T \ln Z$. In the thermodynamic limit, it is more convenient to consider the intensive quantity Ω/V, where V is the volume of space.

The usual GL paradigm dictates that Ω be an analytic function of T and H. Coupled with the symmetry of the problem, one expects that Ω can be expanded as a polynomial of T^2 and H^2 only. However, the known $T^3 \ln T$ specific heat and $H^2 \ln H$ spin susceptibility imply that the GL picture is not good already at fourth order.

Define the dimensionless quantities $t = T/\mu_0$ and $h = H/\mu_0$. On dimensional ground, and with the knowledge that the Sommerfeld expansion cannot generate odd powers of T, one writes down schematically the possible form of Ω, omitting all coefficients:

$$\frac{\Omega}{V} \sim v_\mu k_\mu^4 \{1 + (t^2 + h^2) + F_4(t,h) + \cdots\}. \tag{4}$$

Here the (generalized) fourth-order term F_4 is defined to be the sum of all terms that scale as (energy)^4, up to possible logarithmic dependence. We know that F_4 must be nonanalytic at $T = H = 0$. Its behavior near the origin of the (T,H) plane will depend on the direction of approach. In particular, if one attempts a double expansion of F_4 in t and h, the result will depend on the order in which the expansions are carried out.

D. What is and is not Fermi liquid

First verified by Pethick and Carneiro [4], an oft-repeated observation is that the leading logarithmic correction is a "universal" feature of any FL. This raises the question of what can be considered universal in the expression (4).

We try to address this question in the context of a dilute Fermi gas. The FL is then a low-energy effective theory of the model, with only degrees of freedom near the Fermi surface. One can take a linearized quasiparticle dispersion and an approximated constant density of state around the Fermi surface as the working definition of this effective theory. All the higher-energy modes are integrated out, renormalizing the parameters of this effective theory.

Furthermore, FL is only accurate when all external scales in the problem, such as T and H_a, are dwarfed by the Fermi sea. In other words, μ_0 and k_F should be considered essentially infinite when compared with other scales. This means that, at high enough order, terms in (4) will eventually be deemed infinitesimal and outside the scope of the FL.

For the noninteracting gas, one can calculate Ω exactly. It can be shown that the leading correction to the free gas (second order in t and h) in (4) depends only on the Fermi velocity and

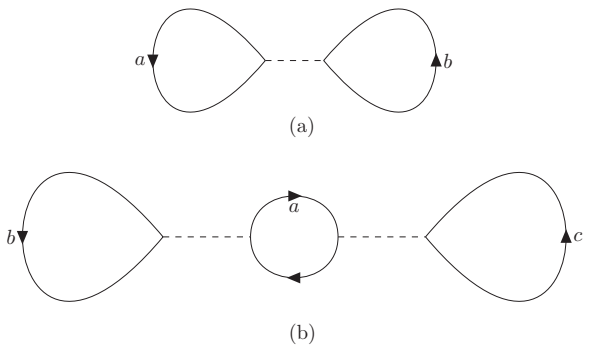

FIG. 3. Hartree-Fock diagrams (a) Ω_1 and (b) Ω_{2b} contributing to the thermodynamic potential up to second order.

density of state at the Fermi surface.[1] So one can conclude that these are within the FL picture, while fourth- and higher-order terms are beyond the FL. In contrast, the nonanalytic terms at fourth order do come from the Fermi surface only, as mentioned above.

To go beyond the dilute limit and perturbation theory, one can replace the Fermi velocity, density of state, and scattering amplitudes of quasiparticles with their fully renormalized values, as suggested in Refs. [13,14]. By construction, this simple replacement yields FL results (second- and third-order terms and the fourth-order logarithmic correction) that remain valid in the strongly interacting regime. This however will not apply to terms outside the scope of the FL and we lose all ability to calculate them in the strongly interacting regime.

III. SOMMERFELD EXPANSION OF Ω FOR FERMI GAS

In this section we take a break from the FL picture and attempt to evaluate the thermodynamic potential of a weakly interacting Fermi gas. This will confirm some assertions made in Sec. II B and also give us some hints at the possible form of F_4.

We wish to calculate the thermodynamic potential of the gas. To second order of perturbation theory, there are three Feynman diagrams to be included. Following the notation of [41], we label these three terms Ω_1, Ω_{2a}, and Ω_{2b}, respectively. Depicted in Fig. 3, Ω_1 and Ω_{2b} are part of the Hartree-Fock approximation and are analytic in T and H. On the other hand, Ω_{2a} as shown in Fig. 2 is both a ring and a ladder diagram and is solely responsible for the nonanalyticity of Ω at this level of approximation.

In this section we will first attempt an expansion in T, writing $\Omega = \alpha_0(H) + \alpha_2(H)t^2 + \cdots$ at finite H. Analytic closed-form solutions of these H-dependent coefficients can be obtained, but we found that it is much more elucidating to further expand each coefficient in a series of H (see Appendix A for more detail).

[1]For the general case of $\mathcal{N}_c > 2$, third-order terms in the magnetic field are possible (see Sec. VI); however, they are also determined exclusively by FL parameters.

To maintain consistency with [41], we define the dimensionless ω via

$$\frac{\Omega}{V} = \frac{k_\mu^3}{6\pi^2}\frac{k_\mu^2}{2m}\sum_{a=1}^{\mathcal{N}_c}\left[\omega_0^{(a)} + (k_\mu a)\sum_{b\neq a}\omega_1^{(ab)} + (k_\mu a)^2\left(\sum_{b\neq a}\omega_{2a}^{(ab)} + \sum_{b\neq a}\sum_{c\neq a}\omega_{2b}^{(abc)}\right) + \cdots\right], \quad (5)$$

where each ω_x originates from the respective Ω_x with the same label. We have temporarily restored $\mathcal{N}_c$ in the above expression. For $\mathcal{N}_c = 2$, the sum over spin is quite trivial and we define the spin-symmetrized version:

$$w_0 = \tfrac{1}{2}(\omega_0^{(\uparrow)} + \omega_0^{(\downarrow)}), \quad (6a)$$

$$w_1 = \tfrac{1}{2}(\omega_1^{(\uparrow\downarrow)} + \omega_1^{(\downarrow\uparrow)}), \quad (6b)$$

$$w_{2a} = \tfrac{1}{2}(\omega_{2a}^{(\uparrow\downarrow)} + \omega_{2a}^{(\downarrow\uparrow)}), \quad (6c)$$

$$w_{2b} = \tfrac{1}{2}(\omega_{2b}^{(\uparrow\downarrow\uparrow)} + \omega_{2b}^{(\downarrow\uparrow\downarrow)}). \quad (6d)$$

A. Free gas and Hartree-Fock contributions

Let $\epsilon(k)$ denote the kinetic energy of free gas, $n_a(x)$ the Fermi function for fermions with spin a, and N_a^0 the noninteracting number density for these fermions:

$$\epsilon(k) \equiv \frac{k^2}{2m}, \quad (7a)$$

$$n_a(k) \equiv (e^{\beta(\epsilon(k)-\mu_a)} + 1)^{-1}, \quad (7b)$$

$$N_a^0 \equiv \int \frac{d^3k}{(2\pi)^3} n_a(k). \quad (7c)$$

The thermodynamic potential of a free gas is given by

$$\frac{\Omega_0}{V} = T\sum_{a=\uparrow,\downarrow}\int \frac{d^3k}{(2\pi)^3}\ln[1 - n_a(k)]. \quad (8)$$

Likewise, the two Hartree-Fock terms Ω_1 and Ω_{2b} are

$$\frac{\Omega_1}{V} = \left(\frac{4\pi a}{m}\right)N_\uparrow^0 N_\downarrow^0, \quad (9)$$

$$\frac{\Omega_{2b}}{V} = \left(\frac{4\pi a}{m}\right)^2\frac{1}{2}\left[\left(\frac{\partial N_\uparrow^0}{\partial\mu_0}\right)N_\downarrow^0 N_\downarrow^0 + \left(\frac{\partial N_\downarrow^0}{\partial\mu_0}\right)N_\uparrow^0 N_\uparrow^0\right]. \quad (10)$$

From here one can identify the associated dimensionless ω_0, ω_1, and ω_{2b}. Up to fourth order in t and h, they are

$$w_0 = -\frac{2}{5} - \frac{\pi^2}{4}t^2 - \frac{1}{16}h^2 + \frac{7\pi^4}{960}t^4 + \frac{1}{1024}h^4 + \frac{\pi^2}{128}t^2h^2, \quad (11a)$$

$$w_1 = \frac{2}{3\pi} + \frac{\pi}{6}t^2 - \frac{1}{4\pi}h^2 + \frac{\pi^3}{40}t^4 + \frac{1}{64\pi}h^4 + \frac{\pi}{16}t^2h^2, \quad (11b)$$

$$w_{2b} = -\frac{4}{3\pi^2} - \frac{5}{18}t^2 - \frac{11}{24\pi^2}h^2 - \frac{17\pi^2}{1440}t^4 + \frac{47}{512\pi^2}h^4 + \frac{35}{192}t^2h^2. \quad (11c)$$

B. Two-bubble diagram Ω_{2a}

The term Ω_{2a} (Fig. 2) is unique among all vacuum diagrams. Depending on how the diagram is arranged, the scattering process involved can be seen as taking place in any one of the three channels: scattering of a particle-hole pair of the same spin, scattering of a particle-hole pair of different spins, and scattering of a particle-particle pair. The first two correspond to the ring and ladder classifications, respectively. The particle-particle Cooper channel is linearly divergent in the UV and we implicitly subtract the diverging part. In the remainder of this section we will consider the diagram exclusively in the ring configuration. Setting $\mathcal{N}_c = 2$, the Feynman diagram in Fig. 2(a) yields

$$\frac{\Omega_{2a}}{V} = -\left(\frac{4\pi a}{m}\right)^2 \int \prod_{i=1}^{3} \frac{d^3\boldsymbol{k}_i}{(2\pi)^3} \times \frac{n_\uparrow(k_1) n_\downarrow(k_2)[n_\uparrow(k_3) + n_\downarrow(k_4)]}{\frac{1}{2m}\left[k_1^2 + k_2^2 - k_3^2 - k_4^2\right]}, \tag{12}$$

where $\boldsymbol{k}_1 + \boldsymbol{k}_2 - \boldsymbol{k}_3 - \boldsymbol{k}_4 = 0$ by momentum conservation.

From here one identifies the quantity w_{2a} as defined in (6):

$$w_{2a}(t,h) = \frac{6\pi^2 m}{k_\mu^7 a^2} \frac{\Omega_{2a}(T,H)}{V}. \tag{13}$$

In [41], this term was examined numerically at $H = 0$. It has the form

$$w_{2a}(t,0) = B + C_1 t^2 + D_1 t^4 \ln t + E_1 t^4 + \cdots. \tag{14}$$

On the other hand, at zero temperature the integral (12) can be done analytically [43], yielding

$$w_{2a}(0,h) = B + C_2 h^2 + D_2 h^4 \ln|h| + E_2 h^4 + \cdots. \tag{15}$$

Next we attempt the double expansion, first in t and then in h. The result is of the form

$$w_{2a}(t,h) = B + C_1 t^2 + C_2 h^2 + f_4(t,h) + (\text{sixth order}), \tag{16}$$

where the fourth-order term f_4 is

$$f_4(t,h) = \frac{1}{2} D_1 t^4 (\ln|h| + \ln\Delta) + D_2 h^4 \ln|h| + F_1 t^4 + E_2 h^4 + F_3 t^2 h^2 + t^4\left[\xi(t,\Delta) + \sum_{i=1}^{\infty} F_{4,i}\left(\frac{t}{h}\right)^{2i}\right]. \tag{17}$$

Here Δ is an infinitesimal infrared cutoff imposed on the momentum transfer $\boldsymbol{q}_r = \boldsymbol{k}_1 - \boldsymbol{k}_3$ to regularize the results. (See Appendix A for the complication of a momentum cutoff.) Apart from the infinitely many $F_{4,i}$, all coefficients appearing in (14), (15), and (17) are given in Table I.

Instead of a nonanalytic $t^4 \ln t$ term, we found $t^4(\ln h + \ln\Delta)$. Going to higher orders in T, we found increasingly singular terms with powers of h and Δ in the denominator, combining to an overall fourth order. We are naturally unable to carry this calculation to infinite order in T, but it is not difficult to infer, using dimensional analysis and symmetry argument, that the h part forms an infinite series of $(t/h)^{2n}$.

In (17), we denote the Δ counterpart of these higher singular terms by $\xi(t,\Delta)$. We made no attempt to infer a general form of ξ, but it is clear that the original integral (12) is finite. One therefore concludes that all infrared divergent terms must resum into a finite quantity, that is,

$$\tfrac{1}{2} D_1 \ln\Delta + \xi(t,\Delta) = \tfrac{1}{2} D_1 \ln t + \kappa, \tag{18}$$

where κ is a constant yet unknown. It will be determined later by matching with the numerical result (14). Note that when one sets t to zero, $f_4(0,h)$ as given in (17) reduces to $D_2 h^4 \ln h + E_2 h^4$, in exact agreement with (15).

By imposing an upper cutoff in $|\boldsymbol{q}_r|$ that is *smaller* than the Fermi momentum, we also verified that the $t^4 \ln h$ term has a contribution only from $2\sqrt{2m\mu_\downarrow} < |q_r| < 2\sqrt{2m\mu_\uparrow}$. That is, it comes from the region where $|q_r| \approx 2k_F$, confirming the earlier claim in the literature [13,14].

The absence of a logarithmic term with the t^2h^2 prefactor in (17) is notable. The accepted wisdom [6] is such that the spin susceptibility *does not* scale as $T^2 \ln T$, which is in line with our result here. Granted, in the present form (17) is only appropriate when $t/h \ll 1$, while spin susceptibility is defined near zero magnetic field. However, the coefficients to the logarithmic terms are robust: Resummation of the series $(t/h)^{2i}$ cannot generate a separate t^2h^2 logarithmic term. If it is absent for $t/h \ll 1$, it must remain so for all values of the ratio.

IV. RESUMMING THE SINGULAR TERMS: FERMI LIQUID PICTURE

The original loop integral (12) is finite when h is set to zero; however, the expression (17) is not even well defined in the same limit. To obtain a well-defined expression for f_4 in this limit, in principle one only needs to swap the order of the h and t expansions. Unfortunately, we cannot analytically evaluate the resultant integrals. Instead, we will identify the $2k_F$ nonanalyticity of (12) with the infrared nonanalyticity of the ladder diagram [Fig. 2(b)] and evaluate the latter exactly within the FL picture.

A. Equivalence between ladder and $2k_F$ nonanalyticity

Historically, the study of nonanalyticity of FL was framed in terms of the quasiparticle self-energy. Amit *et al.* [2] were the first to observe that interaction with a particle-hole pair at either zero or $2k_F$ momentum results in the leading logarithmic correction to the self-energy. In a lengthy paper, Chubokov and Maslov [10] established that the nonanalytic contribution from the scattering of a particle-hole pair at $2k_F$ is exactly equivalent to that of a *particle-particle* pair at zero momentum. Noting that

TABLE I. Coefficients for w_{2a}. The value of E_1 comes from the numerical fit in [41]. The value of κ is determined by Eq. (29).

B	C_1	C_2	D_1	D_2	E_1	E_2	F_1	F_3	κ
$\frac{4(11-2\ln 2)}{35\pi^2}$	$-\ln 2 + \frac{1}{2}$	$-\frac{1+2\ln 2}{8\pi^2}$	$-\frac{\pi^2}{10}$	$\frac{1}{32\pi^2}$	1.62	$\frac{29-102\ln 2}{1536\pi^2}$	$\frac{6597-704\ln 2}{38\,400\pi^2}$	$\frac{19-6\ln 2}{64}$	1.70

the proper self-energy is obtained by differentiating vacuum two-particle-irreducible Feynman diagrams, the above result essentially constitutes a proof that, for our Ω_{2a} term (see Fig. 2), the $|q_l| = 0$ nonanalyticity is equivalent to that of $|q_r| \to 2k_\mu$. Nevertheless, we will offer a stand-alone argument here, applied specifically to Ω_{2a}.

Nonanalyticity of Ω_{2a} must come from where the integrand in (12) is singular at $T = H = 0$. One notes that the denominator of the integrand is proportional to $\boldsymbol{q}_l \cdot \boldsymbol{q}_r$. It may then appear that there are three separate cases: $\boldsymbol{q}_l = 0$, $\boldsymbol{q}_r = 0$, and $\boldsymbol{q}_l \perp \boldsymbol{q}_r$. However, one can find a suitable change of variables such that the integration measure transforms as

$$d^3\boldsymbol{k}_1 d^3\boldsymbol{k}_2 d^3\boldsymbol{k}_3 \to d^3\boldsymbol{q}_r d^3\boldsymbol{q}_l d^3\boldsymbol{X}, \tag{19}$$

where $\boldsymbol{X}$ is some way to represent the remaining three degrees of freedom. It is clear that the vanishing integration measure renders the limits $\boldsymbol{q}_l \to 0$ and $\boldsymbol{q}_r \to 0$ regular by themselves. The only actual singularity is where $\boldsymbol{q}_l$ and $\boldsymbol{q}_r$ are orthogonal to each other.

We have shown at the end of Sec. III B that the nonanalytic terms come from either $|\boldsymbol{q}_r| \to 0$ or $|\boldsymbol{q}_r| \to 2k_\mu$; now we concentrate on the $2k_\mu$ condition. The region of the momentum integration that contributes to the nonanalyticity must then satisfy both the $2k_\mu$ and the orthogonality conditions.

Let us now analyze the part of (12) that is proportional to $n_\uparrow(k_1)n_\downarrow(k_2)n_\uparrow(k_3)$. At zero temperature and magnetic field, these Fermi functions all become the step function, restricting $\boldsymbol{k}_1$, $\boldsymbol{k}_2$, and $\boldsymbol{k}_3$ to within the Fermi sphere. The $2k_\mu$ condition forces $\boldsymbol{k}_1$ and $\boldsymbol{k}_3$ to sit exactly on the Fermi surface and be polar opposites to one another. Note that, by momentum conservation, $\boldsymbol{q}_l = \boldsymbol{k}_3 - \boldsymbol{k}_2$. The orthogonality condition then forces $\boldsymbol{q}_l$ to vanish (see Fig. 4 for illustration). For the other part of (12) where $n_\uparrow(k_3)$ is replaced by $n_\downarrow(k_4)$, one can identify $\boldsymbol{q}_r = \boldsymbol{k}_2 - \boldsymbol{k}_4$ and $\boldsymbol{q}_l = \boldsymbol{k}_1 - \boldsymbol{k}_4$ and the same argument follows.

One can reverse the argument to show that the $\boldsymbol{q}_l \to 2k_\mu$ nonanalyticity is always paired with the limit $\boldsymbol{q}_r \to 0$. It is thus concluded that nonanalyticity of Ω_{2a} comes from the limiting regions of momentum integration where one of $\boldsymbol{q}_r$ and $\boldsymbol{q}_l$ vanishes and the other approaches $2k_\mu$. This can be thought of as a duality between the ring and ladder diagrams (see Fig. 2): The $2k_\mu$ nonanalyticity in the ring form is exactly the zero-momentum nonanalyticity in the ladder form and vice versa.

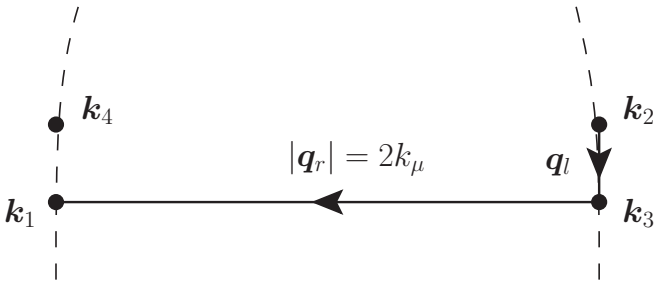

FIG. 4. Configuration from which the $2k_\mu$ nonanalyticity of Ω_{2a} comes. The dashed lines represent the Fermi sphere. The requirements are $|\boldsymbol{q}_r| \to 2k_\mu$, $\boldsymbol{q}_l \perp \boldsymbol{q}_r$, and that $\boldsymbol{k}_1, \ldots, \boldsymbol{k}_3$ lie within the Fermi sphere. Consequently, $\boldsymbol{q}_l$ must vanish and all four momenta $\boldsymbol{k}_1, \ldots, \boldsymbol{k}_4$ must be exactly on the Fermi surface.

Finally, we note that, in either limit, $\boldsymbol{k}_4$ is forced to sit on the Fermi surface too by momentum conservation. Therefore, to capture the nonanalyticity of Ω_{2a}, it suffices to consider the small-momentum limit of both ring and ladder diagrams in Fig. 2, with all four fermion legs restricted to be near the Fermi surface.

B. Ladder diagram and Fermi liquid approximation

Consider the ladder Feynman diagram [Fig. 2(b)], which gives the term Ω_{2a}^{ab} before summing over spins. The Feynman diagram can be understood as the trace of the square of the particle-hole Green's function $\Pi_{ab}(i\nu,q)$, where ν is the bosonic Matsubara frequency. This reduces to Eq. (12) if the full noninteracting form of $\Pi_{\uparrow\downarrow}$ is used.

However, our present goal is to compute all nonanalytic terms *not* coming from $|q_r| \to 0$, and the preceding discussion made clear that one only needs to look at the limit $|\boldsymbol{q}_l| \to 0$, with $\boldsymbol{k}_1, \ldots, \boldsymbol{k}_4$ all near the Fermi surface. One can then employ the asymptotic form of $\Pi_{\uparrow\downarrow}$ for small q, denoted by $\pi_{\uparrow\downarrow}$:

$$\pi_{\uparrow\downarrow}(\varepsilon,q) = \frac{k_\mu^2}{(2\pi)^2 v_\mu}\left\{2 + \frac{\varepsilon}{v_\mu q}\ln\left[\frac{\left(\frac{\varepsilon+H}{v_\mu q}\right)-1}{\left(\frac{\varepsilon+H}{v_\mu q}\right)+1}\right]\right\}. \tag{20}$$

Corrections to this approximated form are introduced as positive powers of $(H/v_\mu k_\mu)^2$, $(T/v_\mu k_\mu)^2$, or $(q/k_\mu)^2$. Since k_μ is to be viewed as an ultraviolet scale of the FL effective theory, these corrections are to be regarded as vanishingly small in the present approximation. It is also not difficult to see that these beyond-FL corrections only yield overall sixth-order terms and higher if they are included in the following calculation.

We define a modified $\tilde{w}_{2a}$ based on w_{2a}, with the full particle-hole bubble $\Pi_{\uparrow\downarrow}$ replaced by $\pi_{\uparrow\downarrow}$:

$$\tilde{w}_{2a}(t,h) = -\left(\frac{24\pi^4}{k_\mu^7 m}\right) T\sum_\nu \int^\Lambda \frac{d^3q}{(2\pi)^3}\,[\pi_{\uparrow\downarrow}(i\nu,q)^2 + \pi_{\downarrow\uparrow}(i\nu,q)^2]. \tag{21}$$

This quantity contains the contribution to w_{2a} coming from the $q_l \to 0$ region of the momentum integral. Due to the small-q approximation, a large-momentum cutoff Λ is necessary to render the expression finite. We assume the hierarchy of scales $v_\mu k_\mu \gg v_\mu \Lambda \gg T, H$.

With a convergence factor $e^{i\omega 0^+}$ appended, the Matsubara frequency sum in (21) can be carried out using standard contour integration tricks. The sum is transformed into an integral over energy ε, weighted by the usual Bose function $n_B(\varepsilon) = (e^{\beta\varepsilon} - 1)^{-1}$, around the branch cut of $\pi_{ab}(\varepsilon,q)^2$ on the real axis. The energy integral only picks up the discontinuity of the integrand across the branch cut, which is precisely the imaginary part. The integration in $\boldsymbol{q}$ can also be carried out.

The end result contains a number of analytic terms: T^4, H^4, T^2H^2, Λ^2T^2, Λ^2H^2, and Λ^4. The cutoff Λ appears here because the omitted large-q processes can nonetheless have small energy and contribute equally well at orders T^2 and H^2. The cutoff dependence signals the incompleteness of our treatment. This nevertheless poses no problem, as we only

want to capture the nonanalytic terms with this approach. The nonanalytic part of (21) reads

$$\tilde{w}_{2a}(t,h) = -\frac{3m^4}{\pi^2 k_\mu^8}\left\{2\int_0^\infty d\varepsilon\, n_B(\varepsilon)\varepsilon^2(\varepsilon+H)\ln\left|\frac{\varepsilon+H}{v_\mu\Lambda}\right| + \int_0^{v_F\Lambda-H} d\varepsilon\, \varepsilon^2(\varepsilon+H)\ln\left|\frac{\varepsilon+H}{v_\mu\Lambda}\right|\right\} + (H\to -H) + (\text{analytic part}). \quad (22)$$

The second term above can be integrated to yield $h^4\ln|H/v_\mu\Lambda|$ plus analytic terms. In addition, one can split $\ln|(\varepsilon+H)/v_\mu\Lambda| = \ln|\varepsilon/v_\mu\Lambda| + \ln|(\varepsilon+H)/\varepsilon|$ in the integrand and notes that

$$\frac{1}{2}D_1 t^4\ln\left(\frac{T}{v_\mu\Lambda}\right) = -\frac{6m^4}{\pi^2 k_\mu^8}\int_0^\infty d\varepsilon\, n_B(\varepsilon)\varepsilon^3\ln\left|\frac{\varepsilon}{v_\mu\Lambda}\right| + (\text{analytic part}). \quad (23)$$

This relation can be used to write $\tilde{w}_{2a}$ in the form

$$\tilde{w}_{2a}(t,h) = \chi(t,h) + \tfrac{1}{2}D_1 t^4\ln t + D_2 h^4\ln h + (\text{analytic part}), \quad (24)$$

where the crossover function $\chi(t,h)$ is defined as

$$\chi(t,h) = -\frac{6m^4}{\pi^2 k_\mu^8}\int_0^\infty d\varepsilon\, n_B(\varepsilon)\varepsilon^2\left[(\varepsilon+H)\ln\left|\frac{\varepsilon+H}{\varepsilon}\right| + (\varepsilon-H)\ln\left|\frac{\varepsilon-H}{\varepsilon}\right|\right]. \quad (25)$$

Expressions (24) and (25) capture *all* the ladder-type nonanalytic terms, which we were unable to obtain to infinite order using the Sommerfeld expansion approach in (17). Indeed, both $t^4\ln t$ and $h^4\ln|h|$ are recovered with correct coefficients.

In order to make a comparison with (16) and (17), one needs to evaluate $\chi(t,h)$ in the limit where the ratio $\alpha = t/h \ll 1$. This is accomplished by expanding the logarithm in (25), assuming ε/H is always small. The expansion is justified because the Bose function $n_B(\varepsilon)$ allows only a contribution from the range $\varepsilon < T$. The result is

$$\chi(t,h) = \frac{1}{2}D_1 t^4\ln\left(\frac{h}{t}\right) + t^4\left[\frac{\pi^4(5-6\gamma_E)+540\zeta'(4)}{120\pi^2} + O(\alpha^2)\right]. \quad (26)$$

One immediately notes that the $\ln|h/t|$ term correctly converts the $\ln t$ in (24) into $\ln|h|$ in the limit $\alpha\to 0$ where h dominates over t.

Finally, one can compare (24) and (26) with (16) and (17) and identify the $O(\alpha^2)$ terms in (26) with the infinite series in (17). This yields

$$\sum_{i=1}^\infty F_{4,i}\alpha^{2i} = \frac{\chi(t,h)}{t^4} + \frac{1}{2}D_1\ln(\alpha) - \left(\frac{\pi^4(5-6\gamma_E)+540\zeta'(4)}{120\pi^2}\right). \quad (27)$$

As an extra check, we computed the coefficient $F_{4,1}$ both using the Sommerfeld expansion and the crossover function $\chi(t,h)$. Both approaches give the identical answer $F_{4,1} = \pi^4/63$.

C. The term Ω_{2a} near the T axis

The infinite series in (17) has been resummed using (27). It is natural to ask if one can now find a well-defined expression for $w(t,h)$ when the ratio α is large.

As it turns out, it is quite tricky to expand $\chi(t,h)$ around a small $1/\alpha$. We relegate the details to Appendix B and note the result here:

$$\chi(t,h) = D_2 h^4\ln\left(\frac{t}{h}\right) - \frac{1}{16}t^2h^2 + h^4\left[\frac{12(\ln 2\pi-\gamma_E)+7}{384\pi^2} + O\left(\frac{1}{\alpha^2}\right)\right]. \quad (28)$$

Equations (27) and (28) can be substituted into (17) to give an expression of $f_4(t,h)$ well defined in the limit of large α. In particular, we are finally in a position to determine the constant κ appearing in (18). Matching the coefficient of t^4 terms, one obtains

$$E_1 = F_1 - \left(\frac{\pi^4(5-6\gamma_E)+540\zeta'(4)}{120\pi^2}\right) + \kappa, \quad (29)$$

which yields $\kappa = 1.51$.

With this final piece of the puzzle found, one has the complete nonanalytic equation of state of a dilute Fermi gas up to overall fourth order in t and h. The fourth-order term $f_4(t,h)$ as defined in (16) is nonanalytic, and its series expansion takes different forms depending on the size of $\alpha = t/h$.

When $\alpha \lesssim 1$, one has

$$f_4(t,h) = \frac{D_1}{2}t^4(\ln h + \ln t) + D_2 h^4\ln h + (F_1+\kappa)t^4 + E_2 h^4 + F_3 t^2h^2 + t^4\sum_{i=1}^\infty (F_{4,i}\alpha^{2i}). \quad (30)$$

The coefficients $F_{4,i}$ for arbitrary i can be computed using (27). Even better, one can just numerically evaluate $\chi(t,h)$ to resum the series.

One can obtain the corresponding expansion for $\alpha \gtrsim 1$ using (28). The result is

$$f_4(t,h) = D_1 t^4\ln t + D_2 h^4\ln t + E_1 t^4 + G_2 h^4 + G_3 t^2h^2 + h^4\sum_{i=1}^\infty (G_{4,i}\alpha^{-2i}), \quad (31)$$

with $G_2 = E_2 + \frac{12(\ln 2\pi-\gamma_E)+7}{384\pi^2}$ and $G_3 = F_3 - \frac{1}{16}$. The infinite series in (31) sums to

$$\sum_{i=1}^\infty G_{4,i}\alpha^{-2i} = \frac{\chi(t,h)}{h^4} - D_2\ln(\alpha) + \frac{1}{16}\alpha^2 - \left[\frac{12(\ln 2\pi-\gamma_E)+7}{384\pi^2}\right]. \quad (32)$$

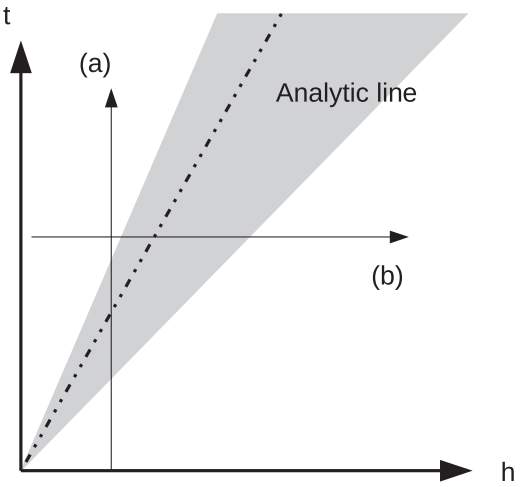

FIG. 5. Sketch of the crossover behavior of the ladder-type nonanalyticity. The shaded crossover region separates the two near-axis areas, where one scale dominates the other. The analytic line in the crossover region is where the two sets of nonanalyticity precisely cancel each other out. The two paths (a) and (b) are discussed in the text.

V. CROSSOVER BEHAVIOR

As discussed in Sec. II B, the ladder-type nonanalyticity [Fig. 2(b)] can be cut off in the infrared by either T or H. The competition between the two scales results in a nontrivial crossover. We sketch the behavior in Fig. 5.

Consider the expression (16) for w. The nonanalytic f_4 term admits two different expansions (30) and (31), good for the regions near the t and h axes in Fig. 5, respectively. When the ratio $\alpha = t/h$ is neither larger nor small, the higher-order terms are important in both expansions and this corresponds to the shaded crossover region. Fortunately, the series can be resummed exactly using (27) and (32).

A. Path (a): Raising t with a fixed h

This is perhaps the scenario most relevant to the experiment. As the effective magnetic field is controlled via the number densities of individual spin components, moving along path (a) in Fig. 5 corresponds to fixing the composition of the gas and tuning the temperature.

In the region near the h axis, Eq. (30) is the appropriate expression to use. To identify the ladder-type nonanalyticity, from the thermodynamic potential one subtracts all the analytic terms and half of the total $t^4 \ln t$ term associated with the ring-type nonanalyticity. The result reads

$$I_a(t,h) = \frac{D_1}{2} t^4 \ln|h| + t^4 \sum_{i=0}^{\infty} F_{4,i} \alpha^{2i}. \tag{33}$$

We have taken the liberty to subtract $D_2 h^4 \ln h$, which is a constant along the path. When α is small, I_a approaches $\frac{D_1}{2} t^4 \ln h$. When α grows large, however, using (27) and (28), one deduces $I_a \sim t^4[\frac{D_1}{2} \ln t + O(\alpha^{-2})]$.

For an intermediate value of α, the crossover can be followed by numerically integrating $\chi(t,h)$. We plot I_a/t^4 against $\ln\alpha$ in Fig. 6(a). The crossover region can be identified from the plot as $0.1 < \alpha < 1$, where the behavior of the function I_a substantially deviates from either asymptotic forms.

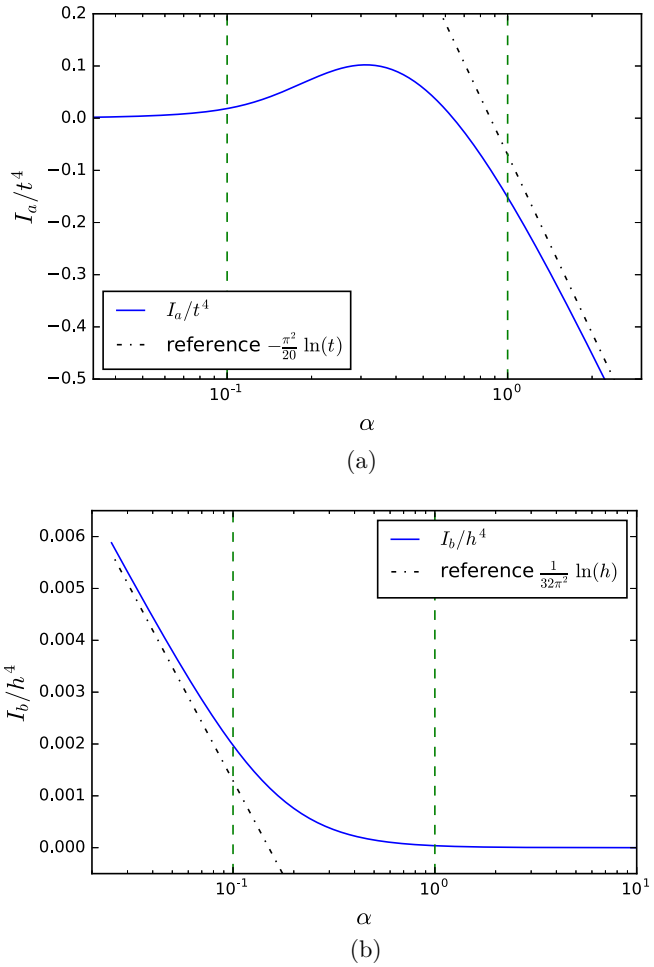

FIG. 6. Plots of the ladder-type nonanalytic parts (a) I_a/t^4 and (b) I_b/h^4 against $\ln\alpha$ up to a vertical offset of (a) $\ln h$ and (b) $\ln t$. The green dashed lines indicate the crossover regions on each plot, corresponding to the shaded area in Fig. 5. Each curve approaches zero on one side of the crossover region, indicating the asymptotic $t^4 \ln h$ and $h^4 \ln t$ behaviors of I_a and I_b, respectively. On the opposite side of the crossover region, I_a and I_b become $t^4 \ln t$ and $h^4 \ln h$, respectively, as indicated by the asymptotically linear behavior.

The result of this section also answers a dangling question from the previous discussion: the fate of the $t^4 \ln t$ behavior in an SU($\mathcal{N}_c$) Fermi gas when the SU($\mathcal{N}_c$) symmetry is broken by unequal number densities of spin components. The ring contribution to the $t^4 \ln t$ term is wholly unaffected, while the ladder contribution remains robust as long as the ratio α is of order unity or bigger.

B. Path (b): Raising h with a fixed t

For completeness, we consider this complementary scenario. The appropriate expansion for f_4 is (31) near the t axis. After subtracting the analytic terms and the $t^4 \ln t$ term for being constant along the path, one obtains the ladder-type

nonanalyticity

$$I_b(t,h) = D_2 h^4 \ln t + h^4 \sum_{i=0}^{\infty} G_{4,i}\alpha^{-2i}. \tag{34}$$

Using (28) and (32), one sees that $I_b \sim h^4[D_2 \ln h + O(\alpha^2)]$ as α gets large. A similar crossover plot of I_b/h^4 against $\ln\alpha$ is presented in Fig. 6(b). The crossover region $0.1 < \alpha < 1$ can be consistently identified from the plot.

C. Analytic line

The analytic line is the most striking feature in Fig. 5, though perhaps also the hardest to access experimentally. Consider the case where one takes both t and h to zero at fixed α. Let us define the Euclidean distance l on the (t,h) plane:

$$l^2 \equiv t^2 + h^2 = h^2(1+\alpha^2) = t^2\left(1+\frac{1}{\alpha^2}\right). \tag{35}$$

It can be shown that χ as given in (25) is of the form $l^4\tilde{\chi}(\alpha)$, where the function $\tilde{\chi}$ is independent of l. Thus the ladder-type nonanalyticity can be cast into the following function:

$$\begin{aligned} I(t,h) &= \chi(t,h) + \frac{D_1}{2}t^4\ln t + D_2 h^4 \ln|h| \\ &= \left[\frac{D_1\alpha^4 + D_2}{(1+\alpha^2)^2}\right] l^4 \ln l + O(l^4). \end{aligned} \tag{36}$$

The $l^4 \ln l$ term vanishes at the special ratio

$$\alpha_c = \pm\sqrt[4]{\left|\frac{D_2}{D_1}\right|} = \pm\sqrt[4]{\frac{8}{5}}\pi. \tag{37}$$

If one approaches $t = h = 0$ along this direction, the thermodynamic potential appears as an entirely analytic function of the distance l and, by extension, of t or h. The two sets of nonanalytic behaviors "cancel" each other out.

D. Away from the dilute limit

The preceding discussion assumes the dilute condition. As we have argued that the logarithmic correction is well within the FL theory, the dilute condition should not be essential for the nonanalytic crossover. We will show that, by replacing the interaction vertices in perturbation theory with the full quasiparticle scattering amplitudes, one can write down the nonanalytic terms in a form that remains valid beyond the dilute limit.

In this section we instead consider a microscopic interaction potential that couples through the particle density (or, conventionally for an electronic system, the charge):

$$\begin{aligned} H_I = \sum_{a,b}\sum_{\boldsymbol{p},\boldsymbol{k},\boldsymbol{q}} \frac{U(|q|)}{2}\psi_a^\dagger\left(\boldsymbol{p}-\frac{\boldsymbol{q}}{2}\right)\psi_b^\dagger\left(\boldsymbol{k}+\frac{\boldsymbol{q}}{2}\right)\psi_b\left(\boldsymbol{k}-\frac{\boldsymbol{q}}{2}\right) \\ \times\psi_a\left(\boldsymbol{p}+\frac{\boldsymbol{q}}{2}\right). \end{aligned} \tag{38}$$

This alternative model directly allows for same-spin scattering. Thus all scattering channels in the full FL phenomenology are already present at first order in perturbation theory and one may directly extrapolate from there. Because of the added possibility of same-spin scattering, Ω_{2a} gains an extra contribution and another vacuum diagram Ω_{2c} contributes to the nonanalyticity at second order, as shown in Fig. 7. We mention in passing that, under the zero-$2k_F$ duality that map ladder and ring diagrams onto each other, this new crescent diagram Ω_{2c} is self-dual.

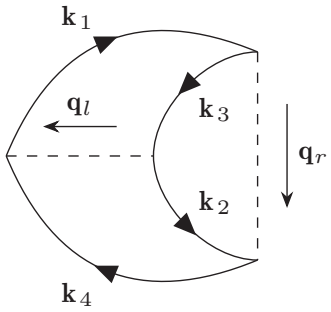

FIG. 7. Feynman diagram corresponding to the new Ω_{2c} term. It is arranged in the unconventional crescent shape to better expose the particle-hole pair structure.

Assuming that $U(|q|)$ is analytic and positive everywhere, the nonanalyticity of Ω_{2a} still comes from the same zero-$2k_F$-momentum-transfer limits and likewise for the new Ω_{2c}. One is then allowed to make the approximation $U(|q_{l,r}|) \approx U(0)$ or $U(2k_\mu)$ where appropriate and write

$$\begin{aligned} \frac{\Omega_{2a}+\Omega_{2c}}{V} = \left(\frac{k_\mu^7 m}{96\pi^4}\right)\{[2U(0)^2 - 2U(0)U(2k_\mu) \\ + U(2k_\mu)^2]\tilde{w}_{2a}(t,0) + U(2k_\mu)^2\tilde{w}_{2a}(t,h)\} \\ + (\text{analytic part}). \end{aligned} \tag{39}$$

The nonanalytic part of $\tilde{w}_{2a}$ is to be identified from Eq. (24).

The so-called fixed-point vertices Γ_s and Γ_c were introduced in [13]. They represent the exact scattering amplitudes of two quasiparticles, where the subscripts s and c stand for the spin and charge channel, respectively. Here we are only interested in the limits where $\boldsymbol{k}_1$ and $\boldsymbol{k}_3$ are either equal or on opposite sides of the Fermi surface. To the lowest order in perturbation theory, the limiting values for the scattering amplitudes are

$$\begin{aligned} \Gamma_c &= \frac{mk_\mu}{\pi^2}\left[U(0) - \frac{1}{2}U(2k_\mu)\right], \\ \Gamma_s &= -\frac{mk_\mu}{\pi^2}\frac{1}{2}U(2k_\mu). \end{aligned} \tag{40}$$

One may now identify $U(0)$ and $U(2k_\mu)$ in (39) with appropriate combinations of Γ_c and Γ_s. Higher-order terms in the perturbation theory will only serve to renormalize the values of k_μ, m, Γ_c, and Γ_s. One then obtains an expression that remains valid outside the dilute regime:

$$\begin{aligned} (\text{nonanalyticity}) = \frac{k_F^5}{96m^*}\left\{\left(\Gamma_s^2+\Gamma_c^2\right)\frac{D_1}{2}t^4\ln t \right. \\ \left. + 2\Gamma_s^2\left(\frac{D_1}{2}t^4\ln t + D_2h^4\ln h + \chi(t,h)\right)\right\}. \end{aligned} \tag{41}$$

As advertised, (41) only depends on parameters in FL theory and should be valid where the FL picture holds. One notes that the crossover is controlled solely by the spin channel, as is intuitively expected.

There are limitations when one wishes to apply (41) to a system beyond the dilute regime. First of all, one loses the ability to calculate the analytic terms at fourth order, which we have shown to mix with the nonanalytic terms during the crossover [see Eqs. (27) and (32)]. Therefore, one no longer has a consistent approximation to the equation of state. Furthermore, while the replacement of the bare interaction vertices with the full scattering amplitudes in (41) is certainly valid, it captures only the so-called backscattering processes. As was shown in Ref. [13], the nonanalyticity receives an additional contribution beyond backscattering.

To leading order in perturbation theory, these neglected contributions come from the small-momentum limit of the third-order Feynman diagrams in Figs. 1(b) and 1(c). The new contributions arise from the region of loop integration where all three particle-hole bubbles are *dynamical*, i.e., frequency dependent. The renormalization of the scattering amplitudes, which is a static effect, cannot account for the new contributions.

We were well justified to drop these terms and retain only the second order Ω_{2a} (Fig. 2) in our initial treatment that assumed dilute conditions. However, these neglected terms can indeed grow to be just as significant as the backscattering processes if the dilute condition no longer holds and they should be considered alongside (41) for a more complete description of the nonanalyticity beyond the dilute regime.

VI. GENERALIZATION TO SU($\mathcal{N}_c$)

When $\mathcal{N}_c > 2$, the additional complexity leads to a rich and exotic phase diagram. However, the mean-field treatment in the existing literature [38,40] by construction yields an analytic expression for the free energy. The nonanalytic effect discussed in the preceding section will qualitatively affect the phase transition [14,21,42].

In this section we give the equation of state including the nonanalytic effect, in the nonmagnetic phase, generalized to $\mathcal{N}_c > 2$. We also propose an experimental scenario that offers the advertised large-$\mathcal{N}_c$ enhancement of the nonanalytic term.

A. Equation of state

It will be convenient to consider the dimensionless magnetic fields $h_a = H_a/\mu_0$. The thermodynamic potential must be SU($\mathcal{N}_c$) symmetric overall. The analytic part can be conveniently expressed in terms of these SU($\mathcal{N}_c$) invariants:

$$S_n \equiv \sum_{a=1}^{\mathcal{N}_c} (h_a)^n, \quad n = 2, \ldots, \mathcal{N}_c. \tag{42}$$

Any $n \geqslant \mathcal{N}_c$ term is a linear combinations of $S_2, \ldots, S_{\mathcal{N}_c}$. The first term S_1 vanishes by the traceless condition. These quantities serve as monomials in a generalized power series expansion.

Generally speaking, $\mathbf{H} \to -\mathbf{H}$ is no longer a symmetry of the model. Thus, starting from S_3, odd terms are allowed in the expansion of the thermodynamic potential. In the treatment of [38,40], the same physics manifests as odd powers of magnetization in the Ginzburg-Landau expansion of free energy.

Up to second order in perturbation theory, the generic expression for the thermodynamic potential (5) is valid for arbitrary $\mathcal{N}_c$. For Ω_0, Ω_1, and Ω_{2b}, the spin sum can still be carried out straightforwardly and the results can be expressed in terms of S_n. In analogy to (6), we define

$$\omega_0 = \frac{1}{\mathcal{N}_c} \sum_{a=1}^{\mathcal{N}_c} \omega_0^{(a)}, \tag{43a}$$

$$\omega_1 = \frac{1}{\mathcal{N}_c(\mathcal{N}_c-1)} \sum_{a=1}^{\mathcal{N}_c} \sum_{b\neq a} \omega_1^{(ab)}, \tag{43b}$$

$$\omega_{2a} = \frac{1}{\mathcal{N}_c(\mathcal{N}_c-1)} \sum_{a=1}^{\mathcal{N}_c} \sum_{b\neq a} \omega_{2a}^{(ab)}, \tag{43c}$$

$$\omega_{2b} = \frac{1}{\mathcal{N}_c(\mathcal{N}_c-1)^2} \sum_{a=1}^{\mathcal{N}_c} \sum_{b\neq a} \sum_{c\neq a} \omega_{2b}^{(abc)}. \tag{43d}$$

Let x denote 0, 1, or $2b$. Up to the fourth overall order in t and h, these quantities have the general form

$$\omega_x = a_0^{(x)} + a_1^{(x)} t^2 + a_2^{(x)} S_2 + a_3^{(x)} S_3 + a_4^{(x)} t^4 + a_5^{(x)} S_4 + a_6^{(x)} (S_2)^2 + a_7^{(x)} t^2 S_2 + \cdots. \tag{44}$$

The coefficients $\{a_i^{(x)}\}$ are summarized in Table II.

For ω_{2a}, it is easier to first withhold the spin sum and consider instead $\omega_{2a}^{(ab)}$ with definite spins a and b. To this end, one defines the centered chemical potential

$$\mu_{ab} = \mu_0 + \tfrac{1}{2}(H_a + H_b), \tag{45}$$

as well as related quantities k_{ab}, v_{ab}, and t_{ab}, where one replaces all occurrences of μ_0 with μ_{ab} in the original definitions. Also, one defines $h_{ab} = (H_a - H_b)/\mu_{ab}$.

Since the dimensionless $\omega_{2a}^{(ab)}$ is symmetric under the exchange of a and b (which is obvious from the Feynman diagrams in Fig. 2), one may rewrite it with explicit spin symmetrization

$$\omega_{2a}^{(ab)} = \frac{12\pi^2 m}{k_\mu^7 a^2} \frac{\Omega_{2a}^{(ab)} + \Omega_{2a}^{(ba)}}{2V}. \tag{46}$$

This nearly coincides with the $\mathcal{N}_c = 2$ spin-symmetrized w_{2a}. However, to adapt the $\mathcal{N}_c = 2$ result, one must replace μ_0 with μ_{ab}, with all the scales and dimensionless parameters modified accordingly. The upshot is

$$\omega_{2a}^{(ab)}(t,h) = \left(\frac{k_{ab}}{k_\mu}\right)^{-7} w_{2a}(t_{ab}, h_{ab}). \tag{47}$$

One may now carry out the spin average over all pairs a and b in (46). While the nonanalytic terms cannot be expressed with the SU($\mathcal{N}_c$) invariants S_n in a simple way, the analytic part can still be summed. The nonanalytic part is not affected

TABLE II. Numerical values of coefficients $a_i^{(x)}$ appearing in Eqs. (44) and (49).

i	$x=0$	$x=1$	$x=2a$	$x=2b$
0	$-\frac{2}{5}$	$\frac{2}{3\pi}$	$\frac{4}{35\pi^2}(11-2\ln 2)$	$-\frac{4}{3\pi^2}$
1	$-\frac{\pi^2}{4}$	$\frac{\pi}{6}$	$\frac{1}{2}(1-2\ln 2)$	$-\frac{5}{18}$
2	$-\frac{3}{4\mathcal{N}_c}$	$\frac{1}{2\pi}\frac{\mathcal{N}_c-4}{\mathcal{N}_c(\mathcal{N}_c-1)}$	$\frac{1}{2\pi^2}\frac{(5\mathcal{N}_c-11)+(-\frac{3}{2}\mathcal{N}_c+1)\ln 2}{\mathcal{N}_c(\mathcal{N}_c-1)}$	$-\frac{1}{6\pi^2}\frac{5\mathcal{N}_c^2-22\mathcal{N}_c+35}{\mathcal{N}_c(\mathcal{N}_c-1)^2}$
3	$-\frac{1}{8\mathcal{N}_c}$	$-\frac{1}{12\pi}\frac{\mathcal{N}_c+8}{\mathcal{N}_c(\mathcal{N}_c-1)}$	$\frac{1}{2\pi^2}\frac{(\mathcal{N}_c-\frac{11}{2})+(-\frac{7}{8}\mathcal{N}_c+\frac{3}{2})\ln 2}{\mathcal{N}_c(\mathcal{N}_c-1)}$	$\frac{1}{12\pi^2}\frac{\mathcal{N}_c^2-2\mathcal{N}_c-35}{\mathcal{N}_c(\mathcal{N}_c-1)^2}$
4	$\frac{7\pi^4}{960}$	$\frac{\pi^3}{40}$	0	$-\frac{17\pi^2}{1440}$
5	$\frac{1}{64\mathcal{N}_c}$	$\frac{1}{32\pi}\frac{1}{\mathcal{N}_c-1}$	$\frac{1}{256\pi^2}\frac{(5\mathcal{N}_c-88)+(-13\mathcal{N}_c+8)\ln 2}{\mathcal{N}_c(\mathcal{N}_c-1)}$	$-\frac{1}{96\pi^2}\frac{\mathcal{N}_c^2-6\mathcal{N}_c+35}{\mathcal{N}_c(\mathcal{N}_c-1)^2}$
6	0	$\frac{3}{32\pi}\frac{1}{\mathcal{N}_c(\mathcal{N}_c-1)}$	$\frac{1}{256\pi^2}\frac{39+9\ln 2}{\mathcal{N}_c(\mathcal{N}_c-1)}$	$-\frac{1}{16\pi^2}\frac{\mathcal{N}_c-16)}{\mathcal{N}_c(\mathcal{N}_c-1)^2}$
7	$-\frac{\pi^2}{32}\frac{1}{\mathcal{N}_c}$	$\frac{\pi}{8}\frac{1}{\mathcal{N}_c-1}$	$\frac{3}{32}\frac{(\mathcal{N}_c-2)(1-\ln 2)}{\mathcal{N}_c(\mathcal{N}_c-1)}$	$-\frac{1}{48}\frac{3\mathcal{N}_c^2-26\mathcal{N}_c+5}{\mathcal{N}_c(\mathcal{N}_c-1)^2}$

by the shift from k_μ to k_{ab} at leading order:

$$\left(\frac{k_{ab}}{k_\mu}\right)^7 f_4(t_{ab},h_{ab}) = f_4(t,h_a-h_b) + (\text{sixth order}). \quad (48)$$

In analogy to (44), the spin-symmetric ω_{2a} can be written as

$$\begin{aligned}\omega_{2a} &= a_0^{(2a)} + a_1^{(2a)}t^2 + a_2^{(2a)}S_2 + a_3^{(2a)}S_3 \\ &\quad + a_5^{(2a)}S_4 + a_6^{(2a)}(S_2)^2 + a_7^{(2a)}t^2S_2 \\ &\quad + \frac{1}{\mathcal{N}_c(\mathcal{N}_c-1)}\sum_a\sum_{b\neq a} f_4(t,h_a-h_b) + \cdots . \end{aligned} \quad (49)$$

The coefficients are also given in Table II. Note that the t^4 term is identically zero in the above expansion.

B. Experimental scenario: $\mathcal{N}_c \to \frac{\mathcal{N}_c}{2} + \frac{\mathcal{N}_c}{2}$

We consider the experimental setup that forbids transitions among SU($\mathcal{N}_c$) spin states. However, the SU($\mathcal{N}_c$) symmetry is still broken by the unequal densities of spin components, which is equivalent to a nonzero generalized magnetic field in our model.

To observe the nonanalytic crossover, a magnetic field is obviously needed, yet we hope for an enhancement of the nonanalytic effect, which receives "extra copies" of the same contribution due to the unbroken part of the symmetry. The simplest scenario works best to fulfill the requirements: We will consider $\mathcal{N}_c$ even and the SU($\mathcal{N}_c$) being broken neatly into SU($\frac{\mathcal{N}_c}{2}$) × SU($\frac{\mathcal{N}_c}{2}$). This corresponds to the effective magnetic fields

$$H_a = \begin{cases} H/2, & a \leqslant \frac{\mathcal{N}_c}{2} \\ -H/2, & a > \frac{\mathcal{N}_c}{2}. \end{cases} \quad (50)$$

This particular scenario closely resembles the spin-$\frac{1}{2}$ electron gas and offers the largest enhancement of the nonanalytic terms.

Let $h = H/\mu_0$, similarly to the $\mathcal{N}_c = 2$ case. In this particular scenario, the SU($\mathcal{N}_c$)-invariant S_n defined in (42) becomes

$$S_n = \begin{cases} \mathcal{N}_c\left(\frac{h}{2}\right)^n & \text{for } n \text{ even} \\ 0 & \text{for } n \text{ odd}. \end{cases} \quad (51)$$

The odd power terms vanish identically due to the restored $H \to -H$ symmetry.

One can substitute (51) into (44) and (49) to recover the equation of state. The full expression is very long and we will not print it here, but we point out the nonanalytic part of Ω_{2a}:

$$\begin{aligned}&\sum_a\sum_{b\neq a} f_4(t,h_a-h_b) \\ &\quad = \frac{\mathcal{N}_c(\mathcal{N}_c-2)}{2} f_4(t,0) + \frac{\mathcal{N}_c^2}{2} f_4(t,h). \end{aligned} \quad (52)$$

Both terms are proportional to $\mathcal{N}_c^2$, compared with the linear scaling of the noninteracting part. This is the potential large-$\mathcal{N}_c$ enhancement that we hope can make the experimental detection of the nonanalytic behaviors less difficult.

C. Hartree-Fock resummation

The above argument for the large-$\mathcal{N}_c$ enhancement is flawed, however. From Table II one can see that both ω_1 and ω_{2b} scale as $O(1)$ when $\mathcal{N}_c$ is large. After spin sum, Ω_1 also scales as $O(\mathcal{N}_c^2)$, while Ω_{2b} is $O(\mathcal{N}_c^3)$.

Since we have been advocating the large-$\mathcal{N}_c$ enhancement, one may question if this does not actually make Ω_{2a} *less* visible in an experiment. In fact, at each order of perturbation theory, the diagrams that form parts of the Hartree-Fock approximation are always proportional to the highest possible power of $\mathcal{N}_c$. As an alternative, we propose that the Hartree-Fock terms may be resummed using a scheme inspired by the familiar Luttinger-Ward (LW) functional [44].

The lowest-order skeleton diagram for the LW scheme coincides with the diagram for Ω_1 [Fig. 3(a)]. If one chooses to include only this diagram, the LW scheme produces only a spin-dependent constant shift σ_a on top of the chemical potential μ_a. We will denote the resultant (approximated) thermodynamic potential by $\Omega_{\rm HF}$,

$$\begin{aligned}\frac{\Omega_{\rm HF}}{V} &= \left(\frac{mT}{2\pi}\right)^{3/2}\sum_a [T\,\mathrm{Li}_{5/2}(-e^{\beta(\mu_0+H_a-\sigma_a)}) \\ &\quad + \frac{1}{2}\sigma_a \mathrm{Li}_{3/2}(-e^{\beta(\mu_0+H_a-\sigma_a)})], \end{aligned} \quad (53)$$

where Li_s is the polylogarithm.

The usual stationary condition for the Luttinger-Ward functional yields a self-consistent condition of the energy shifts:

$$\sigma_a = -\frac{4\pi a}{m}\left(\frac{mT}{2\pi}\right)^{3/2}\sum_{b\neq a}\mathrm{Li}_{3/2}(-e^{\beta(\mu_0+H_b-\sigma_b)}). \quad (54)$$

The above approximation exactly resums the Hartree-Fock self-energy to all orders in perturbation theory, thus the subscript HF. One can add to $\Omega_{\rm HF}$ any beyond-HF vacuum diagram to further refine the approximation. In particular, we wish to write

$$\Omega \approx \Omega_{\rm HF} + \Omega_{2a} + O((k_\mu a)^3). \quad (55)$$

We keep the perturbative power counting for beyond-Hartree-Fock corrections, despite the resummation leading to $\Omega_{\rm HF}$ being already nonperturbative.

Experimentally, one may already solve (54) using the measured values of T, μ_0, and H_a. Then one can calculate $\Omega_{\rm HF}$ from (53) and subtract it from the measured value of Ω to expose Ω_{2a}. However, we propose a further approximation scheme that simplifies the analysis.

First, one notes that N_a, the physical number density of spin a, satisfies the following relation:

$$N_a = -\left(\frac{mT}{2\pi}\right)^{3/2}\mathrm{Li}_{3/2}(-e^{\beta(\mu_0+H_b-\sigma_b)}) + O((k_\mu a)^2). \quad (56)$$

Comparing this equation with (54) and dropping the correction terms on the right-hand side of (56), one may make the approximation

$$\sigma_a \approx \frac{4\pi a}{m}\sum_{b\neq a} N_b. \quad (57)$$

Then $\Omega_{\rm HF}$ can be approximated as

$$\frac{\Omega_{\rm HF}}{V} \approx \sum_{a=1}^{\mathcal{N}_c}\left[\left(\frac{mT}{2\pi}\right)^{3/2} T\,\mathrm{Li}_{5/2}(-e^{\beta(\mu_0+H_a-\sigma_a)}) - \frac{\sigma_a N_a}{2}\right]. \quad (58)$$

This approximation does away with the transcendental equation (54). Crucially, the error introduced to $\Omega_{\rm HF}$ is only $O((k_\mu a)^3)$. Therefore, Eq. (55) remains valid and can be used to identify Ω_{2a} experimentally.

For the present scenario (50), the number density of each spin component must satisfy

$$N_a = \begin{cases} N_0 + \frac{\Delta N}{2} & \text{for } a \leqslant \frac{\mathcal{N}_c}{2} \\ N_0 - \frac{\Delta N}{2} & \text{otherwise.} \end{cases} \quad (59)$$

Then the self-energy shift (57) becomes

$$\sigma_a \approx \begin{cases} \frac{4\pi a}{m}\left[(\mathcal{N}_c-1)N_0 - \frac{\Delta N}{2}\right] \equiv \sigma_\uparrow & \text{for } a \leqslant \frac{\mathcal{N}_c}{2} \\ \frac{4\pi a}{m}\left[(\mathcal{N}_c-1)N_0 + \frac{\Delta N}{2}\right] \equiv \sigma_\downarrow & \text{otherwise} \end{cases} \quad (60)$$

and $\Omega_{\rm HF}$ is

$$\frac{\Omega_{\rm HF}}{V} \approx \frac{\mathcal{N}_c}{2}\left\{\left(\frac{m}{2\pi}\right)^{3/2} T^{5/2}[\mathrm{Li}_{5/2}(-e^{\beta(\mu_0+H/2-\sigma_\uparrow)}) + \mathrm{Li}_{5/2}(-e^{\beta(\mu_0-H/2-\sigma_\downarrow)})] - \frac{4\pi a}{m}\left[(\mathcal{N}_c-1)N_0^2 - \frac{\Delta N^2}{4}\right]\right\}. \quad (61)$$

One notes that the dangerous $\mathcal{N}_c^3$ terms are effectively resummed into the polylogarithms.

After resumming Hartree-Fock diagrams to all orders with the above procedure, Ω_{2a} is precisely the next-leading-order correction. Using Eqs. (46) and (49), up to fourth overall order,

$$\frac{\Omega_{2a}}{V} \approx \frac{k_\mu^7 a^2}{12m\pi^2}\left\{\mathcal{N}_c(\mathcal{N}_c-1)\left[a_0^{(2a)} + a_1^{(2a)}t^2 + a_2^{2a}\frac{\mathcal{N}_c}{4}h^2 + \left(a_5^{(2a)}\frac{\mathcal{N}_c}{16} + a_6^{(2a)}\frac{\mathcal{N}_c^2}{16}\right)h^4 + a_7^{(2a)}\frac{\mathcal{N}_c}{4}t^2h^2\right] + \mathcal{N}_c\left(\frac{\mathcal{N}_c}{2}-1\right)f_4(t,0) + \frac{\mathcal{N}_c^2}{2}f_4(t,h)\right\}. \quad (62)$$

The sum of $\Omega_{\rm HF}$ and Ω_{2a} gives the desired approximation to the thermodynamic potential.

The Ω_{2a} term is $O(\mathcal{N}_c^2)$. For $\mathcal{N}_c > 2$, this brings its size closer to the dominating free-gas contribution, which only scales as $O(\mathcal{N}_c)$. This is the advertised large-$\mathcal{N}_c$ enhancement, and we hope that this will make the quantitative measurement of the nonanalyticity less difficult.

VII. DISCUSSION AND CONCLUSION

We have presented the equation of state for an SU($\mathcal{N}_c$) Fermi gas that can in principle be tested in a cold-atom experiment setup. We found that the thermodynamic potential Ω depends nonanalytically on temperature T and effective magnetic field $\mathbf{H}$ and displays a crossover behavior as the ratio of T and $\mathbf{H}$ is continuously varied. There is a potential enhancement of this nonanalytic behavior if $\mathcal{N}_c > 2$.

The familiar Ginzburg-Landau paradigm asserts that, away from a phase transition, the thermodynamic behavior of a physical system should be analytic. This is in direct contrast with our result, where the equation of state is nonanalytic for any nonzero strength of interaction. Yet the qualitative behavior seen in Fig. 5, even though only at a higher order, is very much reminiscent of what is seen near a typical GL critical point.

This result should hardly come as a surprise. Recall that much of the GL critical phenomenology rests on one single assertion: a diverging correlation length. The particle-hole pair excitation in our present problem exactly fills the role of infinite-range correlation and this is independent of the interaction strength. In this sense, a FL in the normal phase is always critical in the subleading order.

In order to compute the equation of state, we employed a two-step approach in this paper. Analytic terms up to fourth order in t and h were obtained from considering scattering processes with arbitrary momentum transfer in the dilute Fermi gas, and the nonanalytic terms at fourth overall order were then found by considering only small-momentum scattering processes, with the appropriate asymptotic form for the particle-hole pair Green's function being used instead of the exact form.

One is able to do this because, from the Fermi gas picture, it can be seen that these small-momentum-transfer on-Fermi-surface processes are precisely those contributing to the nonanalyticity. The two steps are thus complementary and between them provide the full answer to the calculation. This also serves

as yet another confirmation of the oft-cited observation that the leading nonanalytic correction is universal to all FLs [4].

Our analysis is limited to second-order perturbation theory. On one hand, cold-atom gas experiments have achieved the dilute regime where this approximation is justified; on the other hand, this approximation allows one to analytically obtain a consistent approximation to the equation of state. So we do not find the limitation too restrictive.

As pointed out by Chubukov and co-workers [13,14], one could carry out the same calculation, but with the fully renormalized quasiparticle dispersion and scattering amplitudes in the Fermi liquid theory. The resultant expression (41) remains valid beyond the dilute regime, as long as the Fermi liquid picture is applicable. However, only the so-called backscattering processes were retained in our original analysis. We justified the exclusion of all other processes as being of higher orders using the dilute condition. When the condition no longer holds, these neglected contributions can indeed grow to be as important. We acknowledge that Eq. (41) is only a partial description of the nonanalyticity beyond the dilute regime.

Experimental confirmation of this nonanalytic behavior will be challenging, to say the least. However, we hope to see closure of this old but interesting problem.

ACKNOWLEDGMENTS

This work was supported by Ministry of Science and Technology of Taiwan under Grant No. MOST-104-2112-M-001-006-MY3. P.T.H. was also supported by Grants No. MOST-106-2811-M-001-002 and No. MOST-107-2811-M-001-004. The authors would like to thank Chi-Ho Cheng for some initial collaboration and input.

APPENDIX A: SOMMERFELD EXPANSION

The original Sommerfeld expansion is concerned with integration of a function $f(\varepsilon)$ of energy ε, weighted by the Fermi function $n_F(\varepsilon) = \frac{1}{e^{\beta\varepsilon}+1}$. One expands the function $f(\varepsilon)$ as a power series of ε and reduces the original integral into the sum of moments of the Fermi function.

In the present work our integration variable is the single-particle momentum $\boldsymbol{k}$, rather than the energy. Assuming $f(k)$ depends only on the magnitude $k = |\boldsymbol{k}|$, we adapt the original procedure into

$$\int d^3\boldsymbol{k}\left[n_a(k) - \Theta\left(\mu_a - \frac{k^2}{2m}\right)\right] f(|k|) = \sum_{n=0}^{\infty} \tau_{2n+2} \int d^3\boldsymbol{k}\, \delta(k - \sqrt{2m\mu_a}) \times \frac{1}{k^2}\left[\left(\frac{m}{k}\frac{\partial}{\partial k}\right)^{2n+1} k f(k)\right], \tag{A1}$$

where n_a is given in (7), Θ is the Heaviside step function, and the coefficient τ_n is defined to be

$$\tau_n = \frac{2m}{(n-1)!}\int_0^\infty d\varepsilon\, n_F(\varepsilon)\varepsilon^{n-a}. \tag{A2}$$

Generally, the procedure outlined above does not commute with a momentum cutoff. Any cutoff must be implemented formally as a weighting function multiplied by the original integrand, and the partial derivatives in (A1) should act on the cutoff function equally. We implemented a sharp cutoff using a Heaviside step function to analyze the origin in the momentum space of nonanalyticity in Ω_{2a}.

APPENDIX B: CROSSOVER FUNCTION χ AT SMALL h

The small-h expansion of χ, given in (28), is quite tricky to derive. Unlike its small-t counterpart, the region where $\varepsilon < H_{ab}$ is not suppressed in the integral. A straight series expansion in h is therefore doomed with infrared divergences.

As the expression (25) is manifestly even in h, one can take $h > 0$. At fixed t, we define

$$c(\lambda) \equiv \frac{1}{t^4}\tilde{\chi}(t,h), \tag{B1}$$

where $\lambda = h/t$. By construction $c(0)$ vanishes. Also, by being an even function, its first derivative at zero $c'(0)$ also vanishes. Our strategy will be to evaluate the second derivative $c''(\lambda)$ and then integrate it twice to get back to c.

First, the ε integral in (25) must be reinterpreted as

$$\int_0^\infty d\varepsilon \to \left(\int_0^{H^-} d\varepsilon + \int_{H^+}^\infty d\varepsilon\right). \tag{B2}$$

This does not affect $c(h)$ in any way, but allows one to interchange the order of ε integration and h differentiation. Also, a convergence factor $x^{-2\epsilon}$ with $\epsilon \to 0^+$ is needed: Even though the end result is itself finite, we will break the integral into multiple (diverging) parts, and the convergence factor consistently regularizes these fictitious divergences. One may then write

$$c''(\lambda) = -\frac{3}{8\pi^2}\int_0^\infty dx\left(\frac{2x^{1-2\epsilon}}{e^x-1} + \frac{2\lambda^2}{e^x-1}\frac{x^{1-2\epsilon}}{x^2-\lambda^2}\right). \tag{B3}$$

The first term in the above integral can be straightforwardly integrated, yielding $-1/8$.

For the second piece, one needs to take x to the complex plane and the path of integration is as shown in Fig. 8. One may complete the contour into a close loop as shown, which integrates to zero identically. The arc at infinity vanishes due to

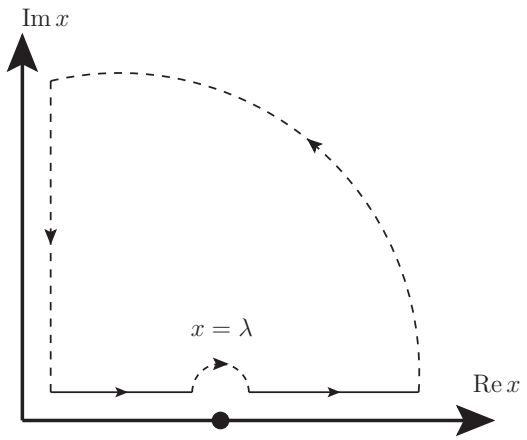

FIG. 8. Contour for (B3). The entire loop integrates to zero, while the solid part is the desired path.

the Bose function. The required c'' is therefore the sum of the small semicircle around $x = \lambda$ and the line integral along the imaginary-x axis. The other necessary trick is to rewrite the Bose function as

$$\frac{1}{e^x - 1} = -\frac{1}{2} + \frac{1}{x} + \sum_{k=1}^{\infty} \frac{2x}{x^2 + (2\pi k)^2} \tag{B4}$$

and carry out the integration term by term.

The small semicircle around the $x = \lambda$ pole is easily evaluated using the residue theorem. With the aforementioned convergence factor $x^{-2\epsilon}$, the integral along the imaginary-x axis and the sum over k can be performed using standard ϵ-expansion and ζ-function regularization techniques, respectively. Individually the pieces in (B4) yield $1/\epsilon$ poles, which cancel among themselves. After taking $\epsilon \to 0$, the end result is

$$c''(\lambda) = -\frac{3}{8\pi^2}\left[\frac{\pi^2}{3} + \lambda^2 \ln|\lambda| + \lambda^2(\gamma_E - \ln 2\pi) + \lambda^2 \sum_{n=1}^{\infty} (-1)^n \zeta(2n+1)\left(\frac{\lambda}{2\pi}\right)^{2n}\right]. \tag{B5}$$

Integrating this result twice with respect to λ and imposing the condition $c(0) = c'(0) = 0$, one recovers (28), as desired.

[1] S. Doniach and S. Engelsberg, Phys. Rev. Lett. **17**, 750 (1966).
[2] D. J. Amit, J. W. Kane, and H. Wagner, Phys. Rev. **175**, 326 (1968).
[3] A. C. Mota, R. P. Platzeck, R. Rapp, and J. C. Wheatley, Phys. Rev. **177**, 266 (1969).
[4] C. J. Pethick and G. M. Carneiro, Phys. Rev. A **7**, 304 (1973).
[5] G. M. Carneiro and C. J. Pethick, Phys. Rev. B **11**, 1106 (1975).
[6] G. M. Carneiro and C. J. Pethick, Phys. Rev. B **16**, 1933 (1977).
[7] D. Belitz, T. R. Kirkpatrick, and T. Vojta, Phys. Rev. B **55**, 9452 (1997).
[8] G. Y. Chitov and A. J. Millis, Phys. Rev. B **64**, 054414 (2001).
[9] S. Misawa, Physica B **294**, 10 (2001).
[10] A. V. Chubukov and D. L. Maslov, Phys. Rev. B **68**, 155113 (2003).
[11] J. Betouras, D. Efremov, and A. Chubukov, Phys. Rev. B **72**, 115112 (2005).
[12] A. V. Chubukov, D. L. Maslov, S. Gangadharaiah, and L. I. Glazman, Phys. Rev. Lett. **95**, 026402 (2005).
[13] A. V. Chubukov, D. L. Maslov, and A. J. Millis, Phys. Rev. B **73**, 045128 (2006).
[14] D. L. Maslov and A. V. Chubukov, Phys. Rev. B **79**, 075112 (2009).
[15] W. R. Abel, A. C. Anderson, W. C. Black, and J. C. Wheatley, Phys. Rev. **147**, 111 (1966).
[16] D. S. Greywall, Phys. Rev. B **27**, 2747 (1983).
[17] D. Coffey and C. J. Pethick, Phys. Rev. B **33**, 7508 (1986).
[18] H. P. van der Meulen, Z. Tarnawski, A. de Visser, J. J. M. Franse, J. A. A. J. Perenboom, D. Althof, and H. van Kempen, Phys. Rev. B **41**, 9352 (1990).
[19] D. Coffey and C. J. Pethick, Phys. Rev. B **37**, 442 (1988).
[20] T. Vojta, D. Belitz, R. Narayanan, and T. Kirkpatrick, Z. Phys. B **103**, 451 (1997).
[21] D. Belitz, T. R. Kirkpatrick, and T. Vojta, Phys. Rev. Lett. **82**, 4707 (1999).
[22] C. Pfleiderer, G. J. McMullan, S. R. Julian, and G. G. Lonzarich, Phys. Rev. B **55**, 8330 (1997).
[23] D. J. Amit, J. W. Kane, and H. Wagner, Phys. Rev. **175**, 313 (1968).
[24] K. S. Dy and C. J. Pethick, Phys. Rev. **185**, 373 (1969).
[25] G. Baym and C. J. Pethick, *Landau Fermi-Liquid Theory: Concepts and Applications* (Wiley-VCH, Weinheim, 1991), p. 216.
[26] G. M. Zhang, Y. H. Su, Z. Y. Lu, Z. Y. Weng, D. H. Lee, and T. Xiang, Europhys. Lett. **86**, 37006 (2009).
[27] X. F. Wang, T. Wu, G. Wu, H. Chen, Y. L. Xie, J. J. Ying, Y. J. Yan, R. H. Liu, and X. H. Chen, Phys. Rev. Lett. **102**, 117005 (2009).
[28] R. Klingeler, N. Leps, I. Hellmann, A. Popa, U. Stockert, C. Hess, V. Kataev, H.-J. Grafe, F. Hammerath, G. Lang, S. Wurmehl, G. Behr, L. Harnagea, S. Singh, and B. Büchner, Phys. Rev. B **81**, 024506 (2010).
[29] M. M. Korshunov, I. Eremin, D. V. Efremov, D. L. Maslov, and A. V. Chubukov, Phys. Rev. Lett. **102**, 236403 (2009).
[30] S. Inouye, M. R. Andrews, J. Stenger, H.-J. Miesner, D. M. Stamper-Kurn, and W. Ketterle, Nature (London) **392**, 151 (1998).
[31] C. Chin, R. Grimm, P. Julienne, and E. Tiesinga, Rev. Mod. Phys. **82**, 1225 (2010).
[32] C.-H. Cheng and S.-K. Yip, Phys. Rev. B **75**, 014526 (2007).
[33] N. Navon, S. Nascimbène, F. Chevy, and C. Salomon, Science **328**, 729 (2010).
[34] M. J. H. Ku, A. T. Sommer, L. W. Cheuk, and M. W. Zwierlein, Science **335**, 563 (2012).
[35] K. Van Houcke, F. Werner, E. Kozik, N. Prokof'ev, B. Svistunov, M. J. H. Ku, A. T. Sommer, L. W. Cheuk, A. Schirotzek, and M. W. Zwierlein, Nat. Phys. **8**, 366 (2012).
[36] R. Desbuquois, T. Yefsah, L. Chomaz, C. Weitenberg, L. Corman, S. Nascimbène, and J. Dalibard, Phys. Rev. Lett. **113**, 020404 (2014).
[37] T. Fukuhara, Y. Takasu, M. Kumakura, and Y. Takahashi, Phys. Rev. Lett. **98**, 030401 (2007).
[38] M. A. Cazalilla, A. F. Ho, and M. Ueda, New J. Phys. **11**, 103033 (2009).
[39] B. J. DeSalvo, M. Yan, P. G. Mickelson, Y. N. Martinez de Escobar, and T. C. Killian, Phys. Rev. Lett. **105**, 030402 (2010).
[40] M. A. Cazalilla and A. M. Rey, Rep. Prog. Phys. **77**, 124401 (2014).
[41] C.-H. Cheng and S.-K. Yip, Phys. Rev. A **95**, 033619 (2017).
[42] D. Belitz, T. R. Kirkpatrick, and T. Vojta, Rev. Mod. Phys. **77**, 579 (2005).
[43] S. Kanno, Prog. Theor. Phys. **44**, 813 (1970).
[44] J. M. Luttinger and J. C. Ward, Phys. Rev. **118**, 1417 (1960).